LIMNOLOGY and OCEANOGRAPHY

ASLO

Limnol. Oceanogr. 66, 2021, 3643–3655

doi: 10.1002/lno.11905

An empirical model to predict methane production in inland water sediment from particular organic matter supply and reactivity

Charlotte Grasset,[1*] **Simone Moras**,[1] **Anastasija Isidorova**,[1] **Raoul-Marie Couture**,[2] **Annika Linkhorst**,[1] **Sebastian Sobek**[1]

[1]Limnology, Department of Ecology and Genetics, Uppsala University, Uppsala, Sweden
[2]Département de Chimie, Université Laval, Québec, Québec, Canada

Abstract

The highest CH_4 production rates can be found in anoxic inland water surface sediments however no model quantifies CH_4 production following fresh particular organic matter (POM) deposition on anoxic sediments. This limits our capability of modeling CH_4 emissions from inland waters to the atmosphere. To generate such a model, we quantified how the POM supply rate and POM reactivity control CH_4 production in anoxic surface sediment, by amending sediment at different frequencies with different quantities of aquatic and terrestrial POM. From the modeled CH_4 production, we derived parameters related to the kinetics and the extent of CH_4 production. We show that the extent of CH_4 production can be well predicted by the quality (i.e., C/N ratio) and the quantity of POM supplied to an anoxic sediment. In particular, within the range of sedimentation rates that can be found in aquatic systems, we show that CH_4 production increases linearly with the quantity of phytoplankton-derived and terrestrially derived POM. A high frequency of POM addition, which is a common situation in natural systems, resulted in higher peaks in CH_4 production rates. This suggests that relationships derived from earlier incubation experiments that added POM only once, may result in underestimation of sediment CH_4 production. Our results quantitatively couple CH_4 production in anoxic surface sediment to POM sedimentation flux, and are therefore useful for the further development of mechanistic models of inland water CH_4 emission.

Inland waters, despite their small global surface, have a strong effect on the greenhouse gas concentration in the atmosphere (Cole et al. 2007; Tranvik et al. 2009). In particular, they can emit large quantities of CH_4 to the atmosphere (Bastviken et al. 2011), a greenhouse gas with 34 times the global warming potential of CO_2 (at 100 yr timescale including climate-carbon feedbacks; Myhre et al. 2013). Most CH_4 is emitted from inland waters via the release of CH_4 bubbles (ebullition), an emission pathway that is highly variable in space and time (DelSontro et al. 2011; Linkhorst et al. 2020; Sieczko et al. 2020). Therefore, the prediction of CH_4 emissions at the ecosystem scale, and in particular of CH_4 ebullition, is very valuable for quantification of the feedback that inland waters can have on climate (Aben et al. 2017; Schmid et al. 2017).

CH_4 ebullition is controlled by physical parameters that regulate the release of CH_4 bubbles (e.g., sediment structure, hydrostatic pressure change; Joyce and Jewell 2003; Scandella et al. 2011; Ramirez et al. 2015; Liu et al. 2016) and by biological processes that regulate CH_4 production in the sediment. Methanogenesis is the final step of the anoxic decomposition of organic matter, and relies on the supply of organic substrates that are fermented into precursors (e.g., acetate or CO_2) for CH_4 production (Valentine et al. 1994). When environmental conditions are favorable for methanogenesis (e.g., anoxic conditions, sediment poor in alternative electron acceptors, and pH close to neutral), CH_4 production will ultimately depend on temperature, particulate organic matter (POM) supply, and POM reactivity (Valentine et al. 1994; Segers 1998).

In marine sediments, which are rich in alternative electron acceptors and typically feature slow sedimentation rates, favorable conditions for methanogenesis are often met in deep and old sediment layers. However, in inland water sediments, such conditions are frequently met already in the upper cm (Sobek et al. 2009). As POM reactivity decreases exponentially with age (Middelburg 1989), methanogenesis decreases with sediment depth, and the highest CH_4 production rates can be found in surface or sub-surface inland water sediments (Clayer et al. 2018;

*Correspondence: charlottemjgrasset@gmail.com

Additional Supporting Information may be found in the online version of this article.

Isidorova et al. 2019). In particular, in inland waters with anoxic bottom waters, most CH_4 will be produced during the first 100 d following POM deposition on the anoxic sediment (Grasset et al. 2018). There are models that correlate CH_4 production with the reactivity or stoichiometry of the organic matter that is present in inland water sediments (Clayer et al. 2018; Isidorova et al. 2019), but these models operate at relatively long time scales and over the whole sediment column. Therefore, these models do not include the fresh and often highly reactive POM that is newly added through sedimentation as a predictor, and thus cannot be used to infer the short-term (< 1 yr) and potentially high CH_4 production rates resulting from new POM reaching the sediments. Several models of CH_4 production at short time-scales exist for peatlands and other wetland ecosystems, but the main components of CH_4 production (e.g., plant primary production, water table level; Potter et al. 2014; Gedney et al. 2019; Grant and Roulet 2002) differ from those of inland waters. A mechanistic model predicting CH_4 production in inland water surface sediments is currently missing, which limits our capability of modeling CH_4 emissions from inland waters to the atmosphere.

The positive relationship between temperature and methanogenesis has been well studied in inland water sediments (Davidson and Janssens 2006; Yvon-Durocher et al. 2014) but the influence of POM supply and reactivity on CH_4 production is less straightforward. This is probably because POM sources are diverse and cover a wide range of reactivity (Kankaala et al. 2003; Duc et al. 2010; West et al. 2012), and because the supply rates are highly variable in space and time (Sobek et al. 2009). POM supply rate depends on the frequency of POM supply to the sediment, and on the quantity of POM added to the sediment within a certain amount of time. Recent studies have shown that CH_4 production rates strongly increase with the quantity of sediment POM (Rodriguez et al. 2018; Berberich et al. 2019). However, no study has investigated the effect that the frequency of POM supply has on CH_4 production in sediments, although the frequency of POM supply can have a significant effect on OM decomposition via modifying microorganism activity and abundance (Hamer and Marschner 2005; Attermeyer et al. 2014). Recent studies have also shown that POM originating from sources that are considered more reactive (e.g., phytoplankton) can have higher CH_4 production rates than POM originating from less reactive sources (e.g., leaves of terrestrial plants; West et al. 2012; Grasset et al. 2018). During aerobic decomposition, POM reactivity decreases exponentially (Boudreau and Ruddick 1991; Koehler and Tranvik 2015), and the time of POM exposure to oxygen before reaching the anoxic sediments is thus also likely to affect anaerobic decomposition rates (Kristensen and Holmer 2001) and CH_4 production. The carbon to nitrogen (C/N) ratio or the total nitrogen (TN) content can serve as a proxy of POM reactivity: a low C/N ratio or a high TN content imply a high content in labile N-rich compounds (e.g., proteins) and a low content in recalcitrant C-rich compounds (e.g., structural compounds; Duarte 1992; Enriquez et al. 1993). Accordingly, studies have shown that the CH_4 production derived from macrophyte detritus or from inland water sediment correlates negatively to the C/N ratio and positively to the TN content (Duc et al. 2010; Grasset et al. 2019; Isidorova et al. 2019). However, there is at present no quantitative relationship that links CH_4 production to POM supply and reactivity across a range of POM sources (e.g., terrestrial and aquatic plants).

Laboratory experiments that measure CH_4 production over time in closed systems can derive parameters related to the extent of POM transformation into CH_4, i.e., the yield of the reaction in units of % or in g of produced CH_4, and to the kinetics of CH_4 production, i.e., the time that it takes to produce a certain amount of CH_4 (Kankaala et al. 2003; Grasset et al. 2018; Grasset et al. 2019). Those parameters can be used to predict CH_4 production rates, i.e., the quantity of CH_4 produced per unit of time. Ultimately, such relationships could be used to model CH_4 bubble formation in anoxic sediments, which is dependent on both the extent and the kinetics of CH_4 production. Indeed, CH_4 porewater concentration can exceed solubility, and CH_4 can form bubbles in the sediment (Algar and Boudreau 2010). As part of the produced CH_4 is lost through oxidation, ebullition or diffusion, CH_4 can only accumulate and form bubbles in the sediment if the CH_4 production rate is higher than the CH_4 loss rate (Schmid et al. 2017; Langenegger et al. 2019).

In this study, we quantified how POM supply rate and POM reactivity control CH_4 production in anoxic surface sediment layers, by experimentally amending sediment at different frequencies with different quantities of aquatic and terrestrial POM. From the modeled CH_4 production, we derived parameters related to the kinetics and the extent of CH_4 production. We hypothesized that in an anoxic sediment, the extent of CH_4 production increases with increasing amount of POM supply and decreasing C/N ratio. We also hypothesized that the extent of CH_4 production within a certain amount of time would not be dependent on the frequency of POM addition, as long as the total amount of added POM is constant. We further hypothesized that CH_4 would be produced more quickly with increasing frequency of POM addition.

Materials and methods

Experimental part

The experimental part consisted of two anoxic incubation experiments. In experiment I, different amounts of POM from three different sources were added to an anoxic sediment one single time (Fig. 1). Prior to the addition to the sediment, the POM from the different sources was pre-aged at oxic conditions for either 1 or 3 weeks, in order to mimic degradation in the water column prior to deposition onto the sediment. Hence this experiment quantified the effect of POM reactivity (3 POM sources, pre-aged 1 or 3 week[s]) and the amount of POM supply (different quantities of POM added) on CH_4 production. In

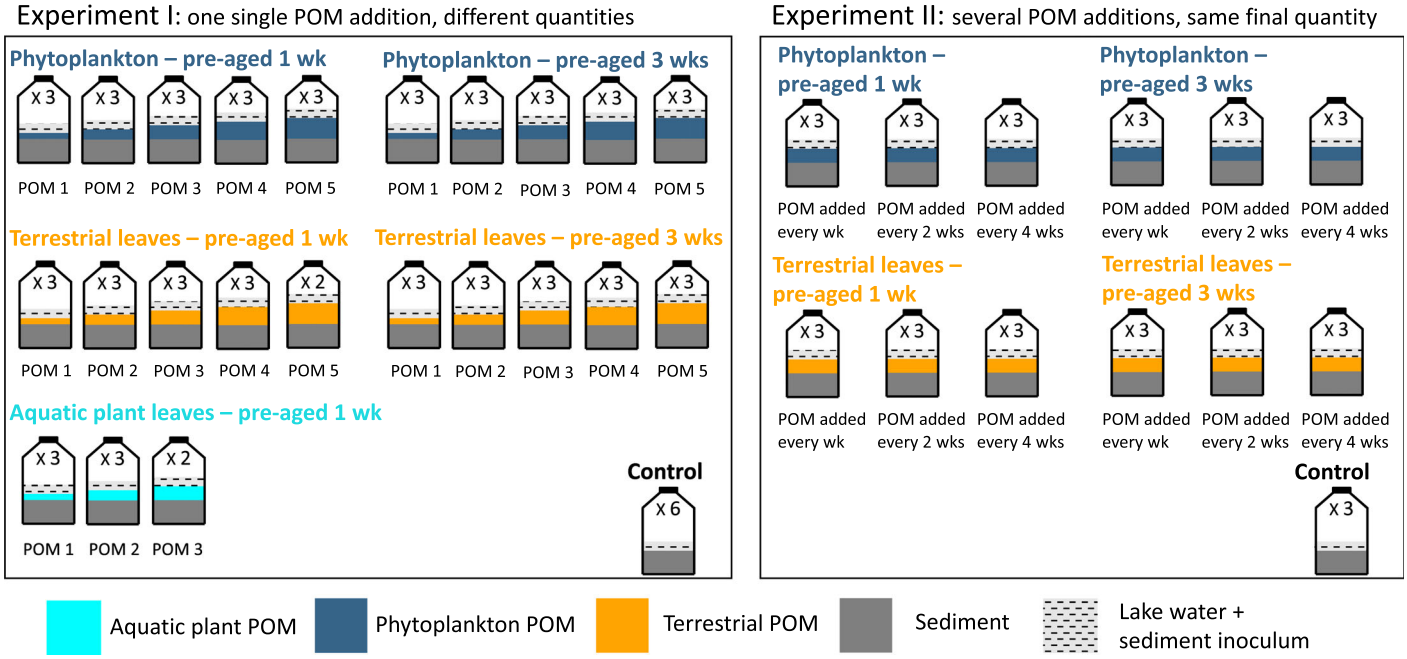

Fig 1. Experimental scheme. In experiment I, different quantities of POM pre-aged for 1 or 3 week(s) were added to a sediment one single time (POM 1 to POM 5 by increasing quantity). In experiment II, POM was added several times during the first 8 weeks to add up to the same total final amount. POM was added in total eight times for the weekly POM addition, four times for bi-weekly addition, and twice for the addition every 4 weeks. See Table S1 for the quantities of POM added in the different treatments.

experiment II, POM from two different sources that was pre-aged for 1 or 3 week(s) was added to an anoxic sediment, adding up to the same total final amount but at different frequencies (POM addition either every 1, 2, or 4 week(s); Fig. 1). POM was added in total eight times for the weekly POM addition, four times for the bi-weekly addition, and twice for the addition every 4 weeks. Hence experiment II quantified the effect of the frequency of POM additions as well as the effect of POM reactivity (2 POM sources, pre-aged 1 or 3 week(s)) on CH_4 production (Fig. 1).

Material sampling and pre-aging

POM sources: Phytoplankton was sampled with a 20 μm net in a small pond in the city of Juiz de Fora (Brazil) during a bloom, and dried at 60°C. The phytoplankton community consisted mainly of cyanobacteria (around 90%) and green algae. A mixture of terrestrial leaves was composed of senescent tree and shrub leaves collected in late autumn in a forest of the city of Uppsala (Sweden) and kept frozen until the start of the experiments. Several individuals of one submerged aquatic plant species (*Elodea canadensis*) were collected at Lake Erken (Sweden) and cultivated in an aquarium until the start of the experiments. The biomass of aquatic plants collected before the start of the experiments was rather low, and limited the material that was available for experiment I (Fig. 1).

CDU sediment: Sediment was sampled with a gravity corer in an oligotrophic drinking water reservoir (Chapéu d'Uvas [CDU], Brazil) in March 2016. The top 5 cm of the sediment were sliced, mixed and stored in a closed bottle in the dark at room temperature, close to in situ temperatures, until the start of the experiments. This sediment was used because previous experiments showed that it provided favorable conditions for methanogenesis (neutral pH, low content in other electron acceptors) and a low TOC content (Grasset et al. 2018; Grasset et al. 2019).

Erken sediment inoculum: Sediment from mesotrophic Lake Erken was also collected shortly (ca. 1–4 weeks) before the start of each incubation experiment (in January 2018 for experiment I and in April 2018 for experiment II) to ensure that an active microbial inoculum would be present in the slurries. The upper 8–10 cm of three sediment cores were mixed together after removing the presumably oxygenated first cm, and kept in a closed bottle at 4°C in the dark until the start of the experiments.

Lake water: Water was also sampled from hard water Lake Erken (mean alkalinity, 1.81 meq L^{-1}), filtered at 0.7 μm using glass fiber filters (Grade GF/F, Whatman, GE Healthcare, UK), and used for dilution of the sediment in the slurries. The water was sampled shortly before the beginning of the experiments (in January 2018) and stored at 4°C.

Chemical analyses of the sampled materials: Sediment and POM sources were dried at 60°C for 24–72 h for total organic carbon (TOC) and TN analysis. Before analysis, samples were manually ground into a fine powder with a mortar and a pestle. About 5 mg of POM, or 30 mg of acidified sediment (with 5% HCl) were encapsulated in tin capsules and analyzed by high-temperature catalytic oxidation with a COSTECH system 4010 elemental analyzer. DOC and TN concentrations of Lake Erken

water were analyzed with a Shimazu analyzer and total phosphorus (TP) was analyzed on a SEAL AutoAnalyzer 3HR (Seal Analytical; DOC of 10 mg L^{-1}, TN of 0.8 mg L^{-1}, and TP of 38 μg L^{-1}).

Aerobic pre-aging of POM: The POM from the different sources was pre-aged through incubation at oxic conditions in the dark at 20°C in 2 L bottles filled with lake water and a diluted sediment inoculum (ca. 0.5 g from CDU and Erken sediment each). The bottles were open and continuously shaken on a rotating table at 50 rpm to ensure oxic conditions, during 1 week for half of them, and during 3 weeks for the other half. After 1 or 3 week(s) of incubation, water was removed from the bottles by centrifugation, and the POM was kept frozen at − 20°C for experiment II, or directly used for experiment I. The relatively short oxic decomposition times of 1 and 3 week(s) were chosen to mimic the time that it can take for detrital POM to be deposited on the sediment surface. The sinking rate of phytoplankton has been estimated on average as 0.64 ± 0.31 m d^{-1} (Bienfang 1981). The sinking time of aquatic plants is expected to be shorter since aquatic plants are mainly found in littoral areas and are denser than phytoplankton. The time for terrestrial POM to reach the sediment is more complex to estimate (longer in case the POM particles resemble large organic flocs, shorter if the POM is attached to mineral particles). In the rest of the manuscript, we refer to POM that has been aerobically decomposed for 1 or 3 week(s) as 1 or 3 week(s) pre-aged.

Anaerobic decomposition of POM

Experiment I: This was a fully factorial experiment that tested the effect of three different factors (quantity of POM addition, POM source, and POM pre-aging) on CH_4 production. The POM from the three different sources, pre-aged 1 or 3 weeks, was added once in triplicates in three to five different quantities (6–274 mg C), to 160 mL glass bottles with 15 g CDU sediment (corresponding to a volume of 12 mL, and an OC content of 2.9%), 40 mL lake water and 0.3 g Erken sediment inoculum (Table S1; Fig. 1). After addition of POM, the slurry OC content varied from 3% to 8%, which is in the same order of magnitude as an average lake sediment OC content (range, 0.5–30%; mean, 5%; (Sobek et al. 2009). If we consider that these single additions correspond to what can be deposited on a sediment over 1 month and that POM is mixed in the upper cm layer, the POM additions correspond to a deposition rate of 5–228 g C m^{-2} per month. This rate is within the same range as the sediment deposition rates given in Sobek et al. (2009; 0.6–110 g C m^{-2} per month). At day 0 of the incubation, the bottles were flushed with N_2, closed with 10 mm thick bromo-butyl septa and aluminum crimps, and flushed again with N_2 for 10 min. The bottles were then flushed with N_2 every week to remove gases or other volatile compounds that could inhibit methanogenesis (Guérin et al. 2008; Magnusson 1993). The bottles remained closed, at 20°C and in the dark until the end of the experiment, which lasted between 52 and 94 d, depending on the time that was needed to observe a plateau in CH_4 production (January 2018–April 2018).

Experiment II: This was a fully factorial experiment that tested the effect of three different factors (frequency of POM addition, POM source, and POM pre-aging) on CH_4 production. The POM from two different sources, pre-aged 1 or 3 week(s), was added several times (3–3.7, 6–7.1, and 12–14.3 mg C of POM added in triplicates every 1, 2, and 4 week(s), respectively) to 160 mL glass bottles with 13 g CDU sediment (corresponding to a volume of 11 mL), 40 mL lake water and 0.3 g Erken sediment inoculum (Table S1; Fig. 1). Thus, the total final amount of POM added in experiment II (between 24 and 28 mg C) corresponded to the second level of POM added in experiment I (POM 2 between 19 and 32 mg C, Table S1). At day 0 of the incubation, the bottles were flushed with N_2, closed and flushed again with N_2 for 10 min. The bottles were then opened in an anaerobic glove box (Belle Technology) for POM additions every 1, 2, or 4 week(s). POM additions were performed during 8 weeks, and the bottles then remained closed, at 20°C and in the dark until the end of the experiment, which lasted ca. 220 d (April 2018–November 2018). All bottles were flushed with N_2 for 10 min every week during the first 8 weeks of the experiment (directly after POM addition), and then three times over the remaining time of the experiment.

Gas concentration measurements

The O_2 concentration was checked in one of the three replicates of each treatment during the anaerobic incubation with an optical sensor system and noninvasive oxygen sensor spots placed in the headspace (Fibox 3 and PSt3, PreSens–Precision Sensing GmbH, Regensburg, Germany). Anoxic conditions (O_2 not detected by the sensor, LOD < 0.03%) were reached after the N_2 flushing at day 0, and maintained during the entire experiments.

CH_4 and CO_2 production were measured bi-weekly in experiment I during the entire incubation, and in experiment II during the first 8 weeks, and then seven times until the end of the experiment. CH_4 and CO_2 production over time were calculated from their respective concentration measured before flushing the headspace with N_2. For CH_4 and CO_2 concentration measurements, 2 mL of the bottle headspace were sampled with a 2.5 mL plastic syringe equipped with a three-way valve and injected into an Ultra-Portable Greenhouse Gas Analyzer (Los Gatos Research Inc., Mountain View, CA) according to Grasset et al. (2018). The gas analyzer was equipped with a gas-tight custom-made sample inlet and a water filter. Ambient air was used as carrier gas, with a CO_2 absorber containing soda lime connected upstream of the inlet, which decreased the CO_2 baseline to ca. 1 ppm. The peaks (concentration in ppm over time) were integrated with the R software, and calibrated against a calibration curve established from dilution series of certified gas standards. The concentrations of the dilution series were cross-checked with a gas chromatograph equipped with a flame ionization detector (FID; Agilent Technologies, 7890 A GC system). The bottles were gently stirred manually while flushing, and we estimated that flushing removed on average 95% of CH_4 and

90% of CO_2 in the headspace and in the water phase. This estimation is based on terrestrial leave samples, pre-aged during 1 week ($n = 14$), in which CH_4 and CO_2 concentrations were measured in the headspace before and directly after flushing at one time point. We assumed that dissolved carbonate concentration remained stable during flushing and that a potential shift of dissolved HCO_3^- towards dissolved CO_2 would be negligible because the concentration of HCO_3^- dominates over that of CO_2 at the pH in the slurries (6.4–6.8). pH was measured at the beginning of the incubation (in the slurry before POM addition) and at the end of the experiment for all samples. The pH increased from 6.4 ± 0.1 to 6.8 ± 0.3 for experiment I and from 6.4 ± 0.1 to 6.6 ± 0.3 for experiment II, and it was assumed to increase linearly during the incubations. The DIC concentration was estimated from the pH, measured CO_2 concentrations in the headspace, and equilibrium constants (Stumm and Morgan 1996). Such estimation is accurate for buffered and non-acidic waters (Abril et al. 2015) such as used in our study (alkalinity of lake Erken: 1.8 meq L^{-1} in January 2018). Total CO_2 (TCO_2) was calculated as the sum of DIC and headspace CO_2. The total CH_4 and TCO_2 production over time (i.e., the total amount of CH_4 and TCO_2 produced at time t) are given in g C. CH_4 production rates are calculated as the slope of CH_4 production increase over time between two flushing events (two measurement points), and are given in g C d^{-1}.

Empirical model of CH_4 production

Total CH_4 production was first modeled for different amounts of POM added one single time according to experiment I. To do so, we fitted a logistic model to the measured total CH_4 production from which we derived parameters related to the kinetics and to the extent of CH_4 production. We tested how CH_4 production can be predicted for different amounts of POM supply and different POM reactivity by testing the correlations between the parameters that describe the extent of CH_4 production, the added POM and the C/N ratio. The model parameters related to the kinetics of CH_4 production were then optimized for POM added at different frequencies according to experiment II.

Logistic model of CH_4 production for different amounts of POM added one single time (experiment I)

The logistic model was fitted to the total CH_4 production after a single POM addition in experiment I (Fig. 1). The anaerobic decomposition of POM is usually divided in three phases (van Hulzen et al. 1999; Vavilin et al. 2008): (1) a lag phase during which alternative electron acceptors with a superior energy gain (than obtained with the reduction of CO_2) are reduced and no CH_4 is produced, (2) an exponential growth phase during which microbial biomass or enzyme concentration are limiting and the total CH_4 production increases exponentially with time, and (3) a last phase during which substrate availability is limiting the total CH_4 production (usually due to a slow hydrolysis). The simple logistic model is often used for modeling the total CH_4 production because it describes well the three phases of CH_4 production for relatively short time scales (incubation time < 50–100 d; Grasset et al. 2019; Kankaala et al. 2003; Vavilin et al. 2008):

$$CH_4(t) = \frac{Asym}{1 + exp[(xmid - t)/scal]} \quad (1)$$

CH_4 (t): total CH_4 production in g C and t: time since the beginning of the incubation in d.

Asym, *xmid*, and *scal* are the model parameters, returned by fitting Eq. 1 to the measured total CH_4 production (Fig. 2):

Asym: the horizontal asymptote at t_∞, in g C. *Asym* thus refers to the extent of CH_4 production (i.e., the yield of the reaction).

xmid: the t value at which CH_4 (t) equals *Asym/2* and corresponds to the length of the lag phase plus the exponential growth phase in d.

scal: the distance on the x-axis between *xmid* and the point where CH_4 (t) equals $Asym/(1+e^{-1})$ in d. *scal* relates to how quickly *Asym*, the asymptote, is reached. *xmid* and *scal* thus refer to the kinetics of CH_4 production, and both are given in d.

We fitted Eq. 1 to the measured data using the nlsList function in the R software (R core Team 2016) to determine the non-linear model parameters for each combination of factors (23 levels: 3–5 POM quantities, 1–2 POM ages and 3 POM sources). The nlsList function was implemented with the logistic self-starting object "SSlogis" that determines the starting estimates for the model parameters of Eq. 1; (nlme package; Pinheiro et al. 2020). A reactivity continuum model was also fitted to the fraction of remaining POM and total CH_4 production and is described in the supplementary material. The logistic model was preferred to the reactivity continuum model because the latter was not able to adequately describe the two

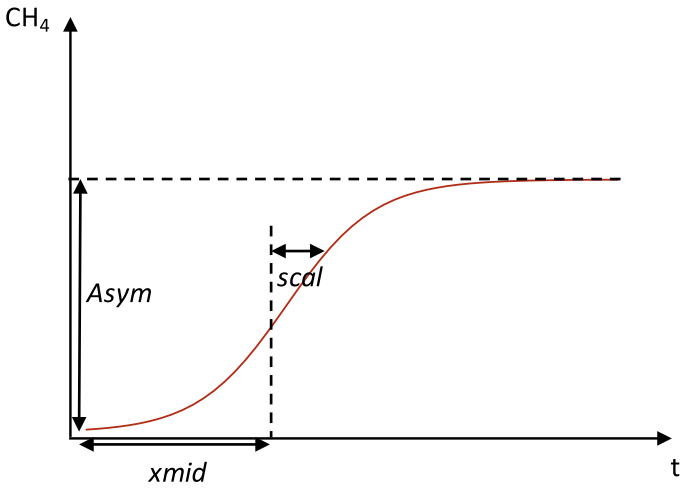

Fig 2. The simple logistic model used to describe CH_4 production using the parameters *Asym*, *xmid*, and *scal* (Pinheiro and Bates 2002), reproduced from Grasset et al. (2019). *Asym* (in g C) refers to the extent of CH_4 production at t_∞ (i.e., the asymptote) while *scal* and *xmid* (in d) relate to the kinetics of CH_4 production.

initial phases of CH_4 production (lag time and exponential growth) and was thus fitted to the total CH_4 production only after removing the first ca. 6–20 d (Figs. S1, S2).

Relationships between CH_4 production, the amount, and the reactivity of POM supply (experiment I)

In order to test if the extent of CH_4 production (*Asym*) can be predicted from different amounts of supplied POM (*added POM*) and POM with different reactivities (C/N ratio), linear regression models were tested using the lm function in R. To this analysis, we added published data from a similar experiment on CH_4 production from 10 different macrophyte species decomposing in an anoxic reservoir sediment at 23°C (Grasset et al. 2019), including POM quantity and C/N ratio. We assumed that the slight difference in temperature of 3°C between the two experiments would not significantly affect the extent of CH_4 production compared to the effect of the experimental treatments.

All statistical analyses and models were carried out using the R software. The models were assessed by visualizing predicted vs. measured values and after examination of the residuals. For the linear relationships between the model parameters total CH_4 production and the amount and reactivity of POM supply, all variables except *scal* were logged (natural logarithm) to normalize distributions.

Calibration of the model describing CH_4 production for POM added at different frequencies (experiment II)

The logistic model as defined above for experiment I was developed from a single POM addition to an anoxic sediment. However, in a natural system, POM is deposited on a sediment at different frequencies and is more likely to continuously fuel CH_4 production. We first assumed that the parameter related to the extent of CH_4 production (*Asym*) was not affected by the frequency of POM addition. To check this assumption, we compared the total CH_4 production at day 219 between the different frequencies of POM addition with the non-parametric Kruskal-Wallis test.

Second, the parameters related to the kinetics of CH_4 production (*xmid* and *scal*) were assumed to change significantly after the second POM addition. We expected a faster CH_4 production due to the suppression of the lag phase (depletion of alternative electron acceptors), and a stimulation of microbial activity and abundance for high frequency additions. We consequently optimized the model derived from experiment I for POM added at different frequencies in experiment II by adjusting the parameters related to the kinetics of CH_4 production (*xmid* and *scal*). We applied the optimization to the first 8 weeks (56 d) when POM was added to the sediment every 7 to 28 d depending on the treatment. Here, CH_4 production rates rather than total CH_4 production were used to optimize the parameters because the production rates are more sensitive to changes in the kinetics of CH_4 production. The predicted CH_4 production rate $P(CH_4)\mathrm{tot}(t)$ in g C d^{-1} for multiple POM additions in experiment II was calculated as the sum of the CH_4 production rates derived from single POM additions as predicted from experiment I. For example, for the treatment with weekly POM additions (POM added at t = 0, 7, 14, 21, 28, 35, 42, 49) between day 0 and day 6:

$$P(CH_4)\mathrm{tot}(t) = P(CH_4)(t)$$

between day 7 and day 13:

$$P(CH_4)\mathrm{tot}(t) = P(CH_4)(t) + P(CH_4)(t-7)$$

between day 49 and day 56:

$$P(CH_4)\mathrm{tot}(t) = P(CH_4)(t) + P(CH_4)(t-7) + \ldots + P(CH_4)(t-49) \quad (2)$$

with $P(CH_4)(t)$ being the predicted CH_4 production rate of a single POM addition at time t in g C d^{-1}, calculated according to the logistic model developed in experiment I.

$P(CH_4)(t)$, was obtained from Eq. 1 after derivation of total CH_4 production according to time:

$$P(CH_4)(t) = \frac{CH_4(t)}{scal} \times \left(1 - \frac{CH_4(t)}{Asym}\right) \quad (3)$$

The model parameter related to the extent of CH_4 production (*Asym*) was predicted according to their linear relationships with *added POM* (Table 1). The parameters related to the kinetics of CH_4 production (*xmid* and *scal*) were given the value obtained for the second level of POM added in experiment I before optimization (POM 2, Tables S1, S2).

Table 1. Relationships between the logistic model parameter related to the extent of CH_4 production (*Asym* in g C), and POM amount (*added POM* in g C) and reactivity (C/N ratio) according to experiment I.

Treatment	Equation	R^2 of the model (*p* value)
All pooled*	ln *Asym* = −1.68 + 0.97 × ln *added POM* − 0.19 × ln C/N	0.97 (< 0.0001)
Phytoplankton 1 week aged	ln *Asym* = −2.26 + 0.87 × ln *added POM*	0.99 (0.0002)
Terrestrial leaves 1 week aged	ln *Asym* = −2.48 + 0.93 × ln *added POM*	1.0 (< 0.0001)
Phytoplankton 3 weeks aged	ln *Asym* = −1.96 + 0.99 × ln *added POM*	1.0 (< 0.0001)
Terrestrial leaves 3 weeks aged	ln *Asym* = −2.74 + 0.93 × ln *added POM*	1.0 (< 0.0001)

Note: To predict CH_4 production rates in experiment II, the regressions between *Asym* and the amount of POM supply for each treatment separately were used.

*This model also include 10 macrophytes that were decomposed in an anoxic reservoir sediment (Grasset et al. 2019).

The predicted CH_4 production rates were optimized using the Nelder and Mead algorithm (Nelder and Mead 1965). The optimization adjusted the parameters related to the kinetics of CH_4 production (*xmid* and *scal*) to obtain the closest fit between predicted and measured CH_4 production rates (i.e., resulting in the lowest residual sum of squares). The best parameters were selected after 100 iterations with random starting parameters ("multiStartoptim" function, mcGlobaloptim package; Moudiki 2013). Furthermore, to visually assess how the optimized parameter sets compare between treatments, the average predicted CH_4 production rates after optimization were calculated with the average of *xmid* and *scal* for the 12 treatments.

Results

Prediction of CH_4 production according to POM reactivity and supply (experiment I)

The logistic model provided a very good fit to the measured total CH_4 production after a single POM addition (experiment I) (R^2 = 0.99; Fig. 3). The extent of CH_4 production (model parameter *Asym*) was strongly and positively correlated with the amount of POM supply and negatively correlated to the C/N ratio of the POM (p value < 0.0001 for both predictors; Fig. 4a and Table 1). The extent of CH_4 production, normalized by the quantity of added POM (*Asym/added POM* in %) decreased significantly and linearly with C/N for POM derived from different sources (phytoplankton, terrestrial and macrophyte POM; Fig. 4b). Pre-aging of POM prior to addition to the sediment did not visibly affect the extent of CH_4 production for phytoplankton, and decreased the extent of CH_4 production for terrestrially derived POM (Fig. 4b). Additionally, when comparing the extent of CH_4 production only between 1 and 3-week (s) pre-aged phytoplankton or only between 1 and 3 week (s) pre-aged terrestrial POM, the extent of CH_4 production did not decrease with the C/N ratio (Fig. 4b).

Calibration of the model describing CH_4 production for POM added at different frequencies (experiment II)

The measured total CH_4 production at day 219 in experiment II was very similar for the different frequencies of POM

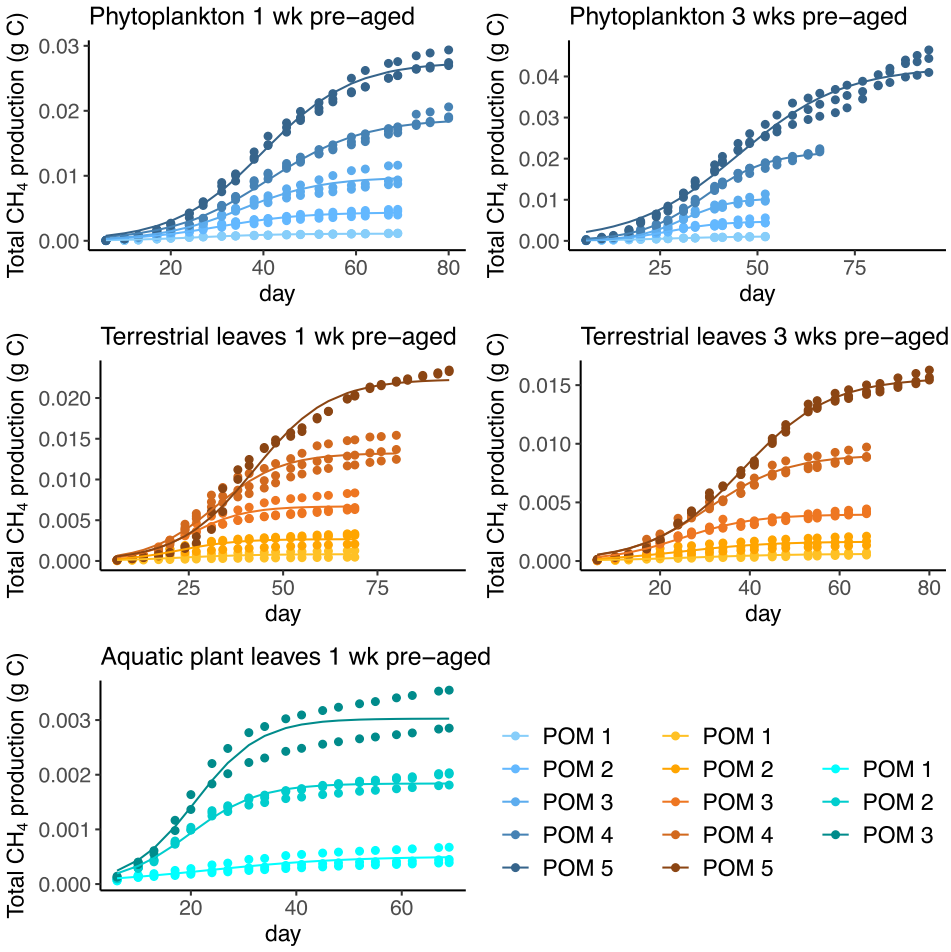

Fig 3. Measured (dots) total CH_4 production during experiment I and fitted logistic model (lines). The legend describes the different amounts of POM added to the sediment, POM 1 being the lowest amount, and POM 5 being the highest (Table S1).

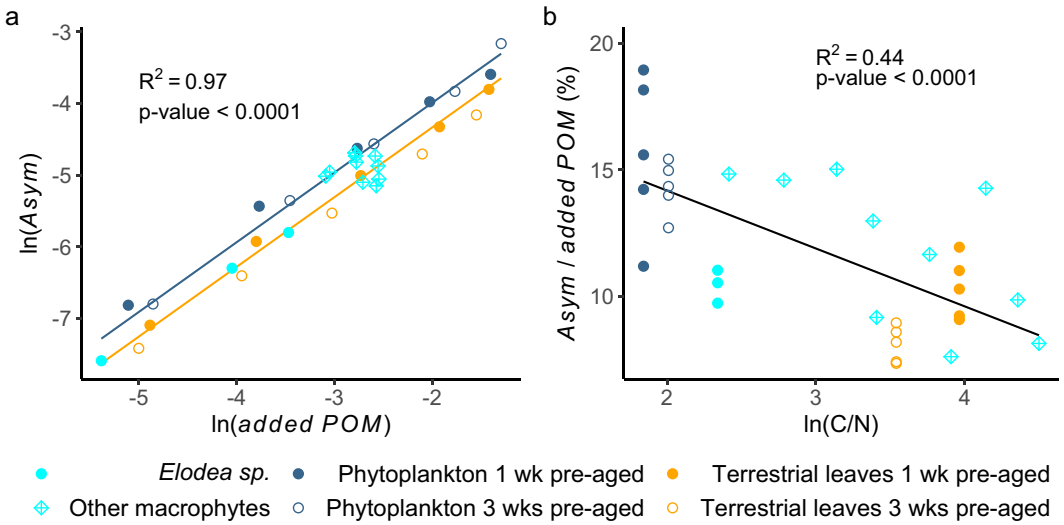

Fig 4. Relationships between the extent of CH_4 production (*Asym*), the amount of added POM in g C, and the C/N ratio. In (**a**), *Asym* (in g C) is represented according to both *added POM* and the C/N ratio (*see* Table 1 for detailed statistics). As *Asym* correlates both to *added POM* and C/N, the regression between *Asym* and *added POM* is represented for two different values of C/N: the average C/N ratio of terrestrial leaves (C/N = 43.6 [34.5–52.7], orange line) and the average C/N ratio of phytoplankton (C/N = 6.9 [6.3–7.5], blue line). In (**b**), *Asym* normalized by *added POM* and given in % (i.e., in g C g C^{-1} × 100) is represented against the C/N ratio. Data from Grasset et al. (2019) (diamonds) was added to the figure and included in the regressions.

Table 2. Measured total CH_4 production at day 219 in experiment II.

Treatment	Measured total CH_4 production at day 219 (%)*
Phytoplankton 1 week pre-aged, every week	26 ± 1
Phytoplankton 1 week pre-aged, every 2 weeks	27 ± 0
Phytoplankton 1 week pre-aged, every 4 weeks	27 ± 1
Phytoplankton 3 weeks pre-aged, every week	30 ± 1
Phytoplankton 3 weeks pre-aged, every 2 weeks	31 ± 2
Phytoplankton 3 weeks pre-aged, every 4 weeks	34 ± 1
Terrestrial leaves 1 week pre-aged, every week	22 ± 1
Terrestrial leaves 1 week pre-aged, every 2 weeks	20 ± 2
Terrestrial leaves 1 week pre-aged, every 4 weeks	20 ± 5
Terrestrial leaves 3 weeks pre-aged, every week	18 ± 1
Terrestrial leaves 3 weeks pre-aged, every 2 weeks	16 ± 2
Terrestrial leaves 3 weeks pre-aged, every 4 weeks	15 ± 1

*The measured total CH_4 production is normalized by *added POM* and given in % (i.e., calculated in g C g C^{-1} × 100).

addition (Table 2, *p* value of the Kruskal–Wallis test > 0.5). The measured rates of CH_4 production with different frequencies of POM addition (experiment II) were poorly predicted by the model derived from a single POM addition (experiment I) (gray lines in Figs. 5, 6). The apparent mismatch between the predicted and measured CH_4 production rates indicated that the model parameters related to the kinetics of CH_4 production (*xmid* and *scal*) strongly differed between experiments I and II (gray lines, Figs. 5, 6). The optimization of *xmid* and *scal* returned better fits (i.e., lower residual sum of squares) between the predicted and measured CH_4 production rates (black lines on Figs. 5, 6). The optimization consistently decreased *xmid* and *scal* (except for 1 out of 12 treatments, Figs. 5, 6). The maximum CH_4 production rate following POM addition was always reached more quickly and was higher than predicted from experiment I. The average predicted CH_4 production rates calculated from the average optimized *xmid* and *scal* for all 12 treatments were also relatively close to the measured CH_4 production rates (pink dashed lines in Figs. 5, 6).

Discussion

Effect of the amount and the reactivity of POM supply on CH_4 production

We propose here the first predictive relationships between the extent of CH_4 production in inland water sediment and the amount and reactivity of POM supplied to the sediment (Fig. 4; Table 1). These relationships may be used for modeling CH_4 production in surface sediments of inland waters. In contrast to other models that predict CH_4 production from properties of already existing sediment (Gebert et al. 2006; Isidorova et al. 2019), the relationships reported here quantify

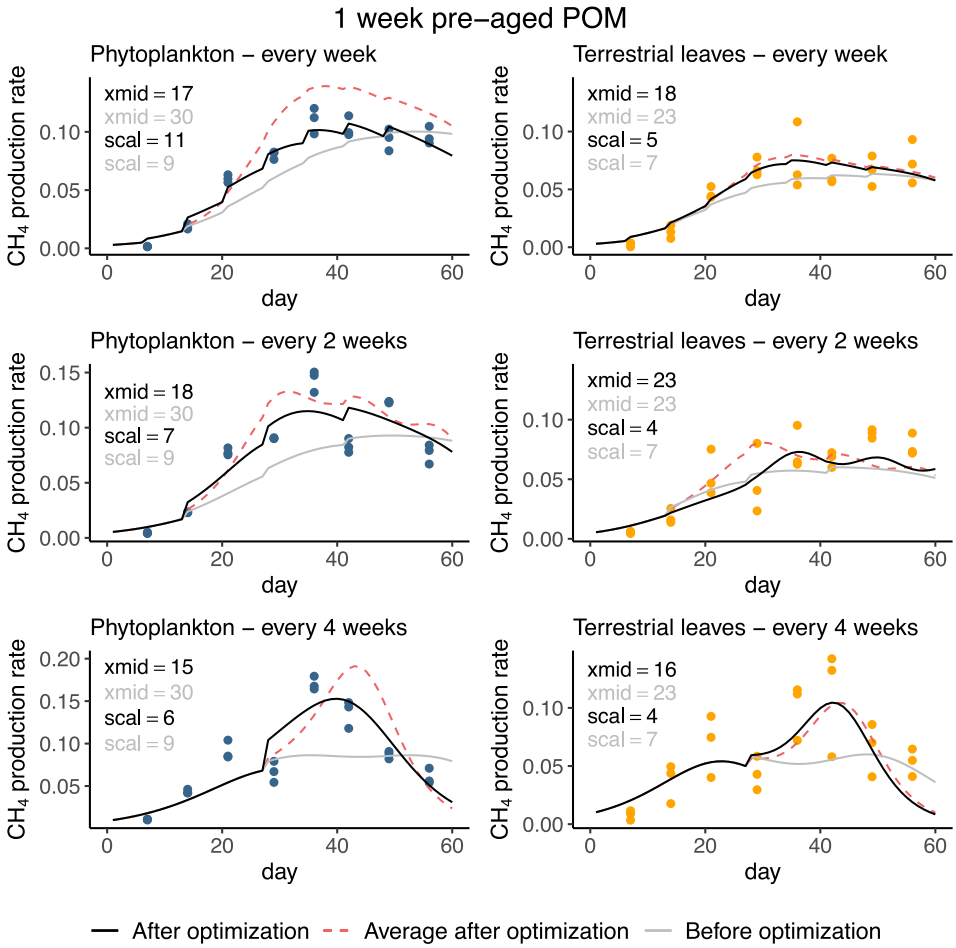

Fig 5. Prediction of CH_4 production rates (mg C d^{-1}) derived from the decomposition of phytoplankton and terrestrial POM, pre-aged during 1 week and added at different frequencies to an anoxic sediment (experiment II). The models are represented by lines while the measurements are represented by dots. CH_4 production rates are predicted according to the logistic model in Eq. 3 before (gray line) and after (black line) optimization of the model parameters *xmid* and *scal* obtained with experiment I. The pink dashed line represents the CH_4 production rates calculated with the average of *xmid* and *scal* after optimization of all 12 treatments (i.e., *xmid* = 17 and *scal* = 4.3).

the response of CH_4 production to new supply of POM from different sources. These relationships can thus be used in biogeochemical inland water models to directly couple CH_4 and sedimentation fluxes. We further note that the data derived from previously published decomposition experiments of 10 different macrophyte species (Grasset et al. 2019) well fitted the data measured in the present experiments with respect to relationships between the C/N ratio, the amount of added POM and the extent of CH_4 production (Fig.4). This is remarkable, since Grasset et al. (2019) studied tropical macrophytes and used a sediment inoculum from tropical lagoons, while here, we used POM from boreal terrestrial and aquatic plants and used sediment inoculum from a boreal lake. This indicates that our relationship might apply to a wide range of different inland waters, but additional studies are nevertheless needed to assess its applicability to different systems with different sediments and POM sources.

As hypothesized, the extent of CH_4 production linearly increased with the amount of supplied POM (Fig. 4a; Table 1). This result suggests that within the range of aquatic and terrestrial OC sedimentation rates that can be found in inland waters, the total CH_4 production increases linearly with the POM deposition rate. However, POM from certain plant species may contain or form compounds (e.g., polyphenols or fatty acids) during its decomposition that can inhibit CH_4 production (Emilson et al. 2018; Grasset et al. 2019). Hence, the relationship that we propose here might not be valid for POM derived from some floating-leaved or emergent species that are rich in polyphenolic compounds (Smolders et al. 2000), or for forest litter rich in phenols (Emilson et al. 2018).

The extent of CH_4 production also linearly decreased with increasing C/N ratio of the POM (Fig. 4b; Table 1), as hypothesized. This confirms similar findings of previous studies (Gebert et al. 2006; Duc et al. 2010; Gebert et al. 2019;

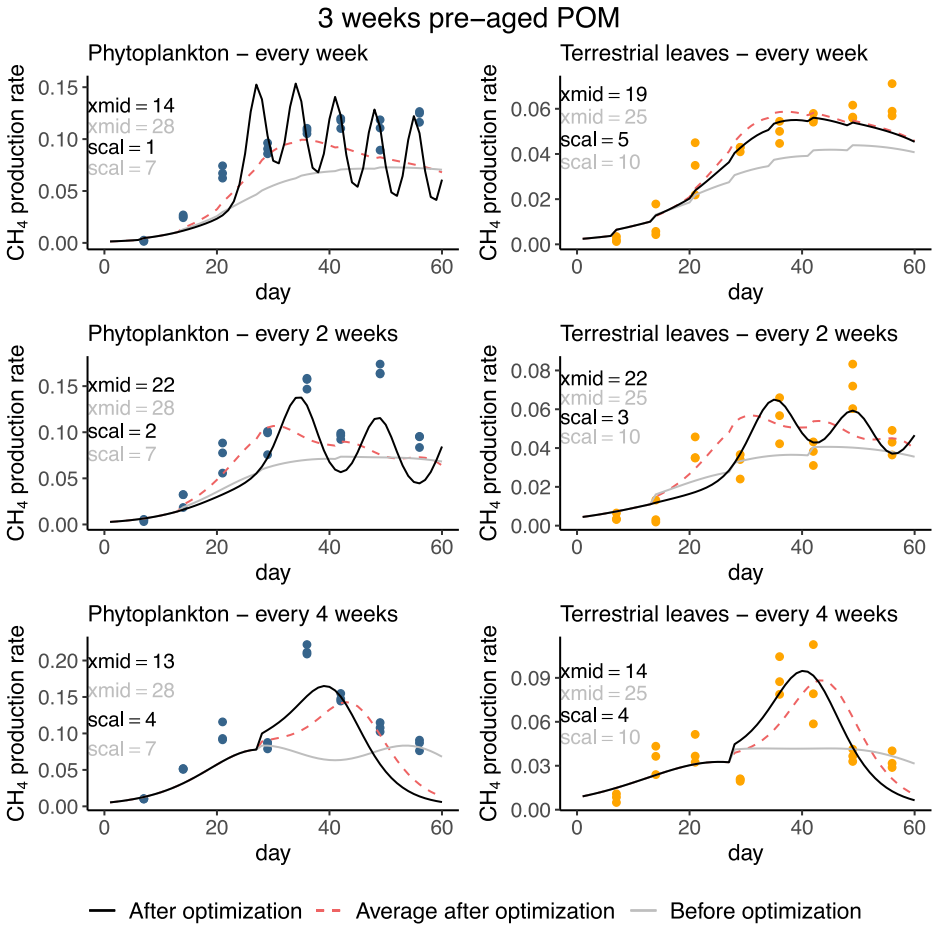

Fig 6. Prediction of CH_4 production rates (mg C d^{-1}) derived from the decomposition of phytoplankton and terrestrial POM, pre-aged during 3 weeks and added at different frequencies to an anoxic sediment (experiment II). The models are represented by lines while the measurements are represented by dots. CH_4 production rates are predicted according to the logistic model in Eq. 3 before (gray line) and after (black line) optimization of the model parameters *xmid* and *scal* obtained with experiment I. The pink dashed line represents the CH_4 production rates as calculated from the average of *xmid* and *scal* after optimization of all 12 treatments (i.e., *xmid* = 17 and *scal* = 4.3).

Isidorova et al. 2019). We show here that the C/N ratio can be used to compare CH_4 production between POM derived from a broad range of different sources (terrestrial leaves, aquatic plant leaves, phytoplankton). However, pre-aging of POM prior to addition to the sediment did not strongly affect the extent of CH_4 production for phytoplankton, despite a higher C/N ratio (and thus a presumably lower reactivity) of the 3 weeks pre-aged phytoplankton-derived POM (Fig. 4b). Furthermore, the POM derived from 3 weeks pre-aged terrestrial leaves had a lower C/N ratio (and thus a presumably higher reactivity), but also a lower extent of CH_4 production than the 1 week pre-aged terrestrial-leave-derived POM (Fig. 4b). Our results consequently suggest that the C/N ratio might not be an accurate proxy of POM reactivity and the extent of CH_4 production at the relatively small-scale changes potentially occurring to the POM within such short time (i.e., a couple of weeks).

Effect of POM supply frequency on CH_4 production

While the frequency of POM addition did not significantly affect the extent of CH_4 production (Table 2), it strongly affected the kinetics of CH_4 production (Figs. 5, 6). In particular, the maximum CH_4 production rate was reached more quickly and was higher than that predicted with the model derived from only one POM addition (Figs. 5, 6). The highest CH_4 production rates (ca 0.1–0.15 mg C d^{-1} corresponding to 46–80 µmol d^{-1} per g C of slurry) were in the same order of magnitude as the highest production rates from other freshwater sediments incubated without POM addition (e.g., ca. 30 µmol d^{-1} g C^{-1} [Isidorova et al. 2019; Praetzel et al. 2020 and ca. 20–40 µmol d^{-1} g OM^{-1} [Berberich et al. 2019). In earlier sediment incubation experiments, POM was typically added to the sediment only one time (e.g., Kankaala et al. 2003; West et al. 2012; Grasset et al. 2018). Our results

indicate that such experiments can accurately predict the extent of POM transformation into CH_4 (Table 2), but they are likely to underestimate peak CH_4 production rates in anoxic sediments (Figs. 5, 6). This is especially important for modeling CH_4 ebullition, because CH_4 can accumulate in the sediment only if CH_4 production rates exceed the rate of CH_4 loss through diffusion, ebullition and oxidation (Schmid et al. 2017; Langenegger et al. 2019). Consequently, underestimating the peak in CH_4 production rate following POM deposition onto a sediment is likely to result in an underestimation of the CH_4 ebullition flux. Interestingly, the average kinetic parameters of the different POM sources in this study returned CH_4 production rates relatively similar to the measured CH_4 production rates (Figs. 5, 6). This suggests that when POM is frequently supplied to the sediment (more often than monthly), the average of the kinetic parameters given in Figs. 5, 6 (i.e., 17 for *xmid* and 4.3 for *scal*) can thus be used to give an approximate prediction of CH_4 production rates for phytoplankton-derived or terrestrially derived POM. Studies are nevertheless needed to further investigate how the kinetic parameters of CH_4 production can vary when POM is added regularly to a sediment, in order to improve this prediction.

Applicability of the model

The equations and parameters derived from our empirical experiments (*Asym* given in Table 1, *xmid* = 17 and *scal* = 4.3) can be used to predict the short-term (< ca. 100 d) CH_4 production rates in anoxic inland water surface sediments, based on POM supply (i.e., POM sedimentation rate) and reactivity (C/N ratio). The CH_4 production rates derived from our model can be directly used to model CH_4 ebullition in combination with physical models that predicts bubble growth and migration through the sediment column (e.g., Ramirez et al. 2015; Scandella et al. 2011). Our results can also be used to model diffusive CH_4 flux from the sediment to the water column, but the limited knowledge on the drivers of CH_4 oxidation is currently limiting the prediction of CH_4 loss during CH_4 diffusion over the sediment and water column.

Several aspects need to be taken into account when using our model to predict CH_4 production. Firstly, in-situ CH_4 production extends beyond the time scale of the experiment, and a substantial part of CH_4 production can occur after 100 d. For example, a study on reservoir sediments has shown that POM can fuel significant CH_4 production for up to 6–12 years for tropical sediments rich in aquatic and terrestrial POM, respectively (Isidorova et al. 2019). For an exhaustive model of CH_4 production in inland water sediments, our short-term model that predicts CH_4 production according to POM supply and reactivity should consequently be completed by a long-term model of CH_4 production during sediment diagenesis (e.g., Clayer et al. 2018; Isidorova et al. 2019). Furthermore, our model is directly applicable to inland waters with anoxic bottom waters where POM is decomposed at anoxic condition as soon as it reaches surface sediments. However, in systems with oxygenated bottom water, the aerobic decomposition of POM in the surface sediment needs to be accounted for, and CH_4 production will be lower than reported in our study (Table 2) because the POM has undergone aerobic decomposition in oxygenated surface sediment before reaching anoxic sediment layers. Lastly, our study focused on POM reactivity in terms of intrinsic composition, but POM reactivity is also likely to differ between different sediment matrices with different biological, geochemical and physical characteristics (LaRowe et al. 2020). Further studies should consequently investigate in how far this model applies to different inland water sediments.

References

Aben, R. C. H., and others. 2017. Cross continental increase in methane ebullition under climate change. Nat. Commun. **8**: 1682.

Abril, G., and others. 2015. Technical note: Large overestimation of pCO2 calculated from pH and alkalinity in acidic, organic-rich freshwaters. Biogeosciences **12**: 67–78.

Algar, C. K., and B. P. Boudreau. 2010. Stability of bubbles in a linear elastic medium: Implications for bubble growth in marine sediments. J Geophys Res Atmos **115**: F03012. doi: 10.1029/2009JF001312

Attermeyer, K., and others. 2014. Enhanced bacterial decomposition with increasing addition of autochthonous to allochthonous carbon without any effect on bacterial community composition. Biogeosciences **11**: 1479–1489.

Bastviken, D., L. J. Tranvik, J. A. Downing, P. M. Crill, and A. Enrich-Prast. 2011. Freshwater methane emissions offset the continental carbon sink. Science **331**: 50.

Berberich, M., J. Beaulieu, T. Hamilton, S. Waldo, and I. Buffam. 2019. Spatial variability of sediment methane production and methanogen communities within a eutrophic reservoir: Importance of organic matter source and quantity. Limnol. Oceanogr. **65**: 1336–1358.

Bienfang, P. K. 1981. Sinking rates of heterogeneous, temperate phytoplankton populations. J. Plankton Res. **3**: 235–253.

Boudreau, B. P., and B. R. Ruddick. 1991. On a reactive continuum representation of organic matter diagenesis. Am. J. Sci. **291**: 507–538.

Clayer, F., A. Moritz, Y. Gélinas, A. Tessier, and C. Gobeil. 2018. Modeling the carbon isotope signatures of methane and dissolved inorganic carbon to unravel mineralization pathways in boreal lake sediments. Geochim. Cosmochim. Acta **229**: 36–52.

Cole, J. J., and others. 2007. Plumbing the global carbon cycle: Integrating inland waters into the terrestrial carbon budget. Ecosystems **10**: 172–185.

Davidson, E. A., and I. A. Janssens. 2006. Temperature sensitivity of soil carbon decomposition and feedbacks to climate change. Nature **440**: 165–173.

DelSontro, T., M. J. Kunz, T. Kempter, A. Wüest, B. Wehrli, and D. B. Senn. 2011. Spatial heterogeneity of methane ebullition in a large tropical reservoir. Environ. Sci. Technol. **45**: 9866–9873.

Duarte, C. M. 1992. Nutrient concentration of aquatic plants: Patterns across species. Limnol. Oceanogr. **37**: 882–889.

Duc, N. T., P. Crill, and D. Bastviken. 2010. Implications of temperature and sediment characteristics on methane formation and oxidation in lake sediments. Biogeochemistry **100**: 185–196.

Emilson, E. J. S., and others. 2018. Climate-driven shifts in sediment chemistry enhance methane production in northern lakes. Nat. Commun. **9**: 1801.

Enriquez, S., C. M. Duarte, and K. Sand-Jensen. 1993. Patterns in decomposition rates among photosynthetic organisms: The importance of detritus C-N-P content. Oecologia **94**: 457–471.

Gebert, J., C. Knoblauch, and A. Gröngröft. 2019. Gas production from dredged sediment. Waste Manag. **85**: 82–89.

Gebert, J., H. Köthe, and A. Gröngröft. 2006. Prognosis of methane formation by river sediments (9 pp). J. Soil. Sediment. **6**: 75–83.

Gedney, N., C. Huntingford, E. Comyn-Platt, and A. Wiltshire. 2019. Significant feedbacks of wetland methane release on climate change and the causes of their uncertainty. Environ. Res. Lett. **14**: 084027.

Grant, R. F., and N. T. Roulet. 2002. Methane efflux from boreal wetlands: Theory and testing of the ecosystem model Ecosys with chamber and tower flux measurements. Glob. Biogeochem. Cycle **16**(4): 2-1–2-16.

Grasset, C., G. Abril, R. Mendonça, F. Roland, and S. Sobek. 2019. The transformation of macrophyte-derived organic matter to methane relates to plant water and nutrient contents. Limnol. Oceanogr. **64**: 1737–1749.

Grasset, C., R. Mendonça, G. Villamor Saucedo, D. Bastviken, F. Roland, and S. Sobek. 2018. Large but variable methane production in anoxic freshwater sediment upon addition of allochthonous and autochthonous organic matter. Limnol. Oceanogr. **63**: 1488–1501.

Guérin, F., G. Abril, A. de Junet, and M. P. Bonnet. 2008. Anaerobic decomposition of tropical soils and plant material: Implication for the CO2 and CH4 budget of the petit Saut reservoir. Appl. Geochem. **23**: 2272–2283.

Hamer, U., and B. Marschner. 2005. Priming effects in soils after combined and repeated substrate additions. Geoderma **128**: 38–51.

Isidorova, A., C. Grasset, R. Mendonça, and S. Sobek. 2019. Methane formation in tropical reservoirs predicted from sediment age and nitrogen. Sci. Rep. **9**: 11017.

Joyce, J., and P. W. Jewell. 2003. Physical controls on methane ebullition from reservoirs and lakes. Environ. Eng. Geosci. **9**: 167–178.

Kankaala, P., T. Kaki, and A. Ojala. 2003. Quality of detritus impacts on spatial variation of methane emissions from littoral sediment of a boreal lake. Archiv Fur Hydrobiol **157**: 47–66.

Koehler, B., and L. J. Tranvik. 2015. Reactivity continuum modeling of leaf, root, and wood decomposition across biomes. J. Geophys. Res. Biogeo. **120**: 1196–1214.

Kristensen, E., and M. Holmer. 2001. Decomposition of plant materials in marine sediment exposed to different electron acceptors (O2, NO3−, and SO42−), with emphasis on substrate origin, degradation kinetics, and the role of bioturbation. Geochim. Cosmochim. Acta **65**: 419–433.

Langenegger, T., D. Vachon, D. Donis, and D. McGinnis. 2019. What the bubble knows: Lake methane dynamics revealed by sediment gas bubble composition. Limnol. Oceanogr. **64**: 1526–1544.

LaRowe, D. E., and others. 2020. The fate of organic carbon in marine sediments - new insights from recent data and analysis. Earth-Sci Rev **204**: 103146.

Linkhorst, A., and others. 2020. Comparing methane ebullition variability across space and time in a Brazilian reservoir. Limnol. Oceanogr. **65**: 1623–1634.

Liu, L., J. Wilkinson, K. Koca, C. Buchmann, and A. Lorke. 2016. The role of sediment structure in gas bubble storage and release. J. Geophys. Res. Biogeosci. **121**: 1992–2005.

Magnusson, T. 1993. Carbon dioxide and methane formation in forest mineral and peat soils during aerobic and anaerobic incubations. Soil Biol. Biochem. **25**: 877–883.

Middelburg, J. J. 1989. A simple rate model for organic matter decomposition in marine sediments. Geochim. Cosmochim. Acta **53**: 1577–1581.

Moudiki, T. 2013. mcGlobaloptim: Global optimization using Monte Carlo and Quasi Monte Carlo simulation. R package version 0.1.

Myhre, G. and others 2013. Anthropogenic and Natural Radiative Forcing. *In* T. F. Stocker and others [eds.], Climate Change 2013: The Physical Science Basis. Contribution of Working Group I to the Fifth Assessment Report of the Intergovernmental Panel on Climate Change. Cambridge Univ. Press.

Nelder, J. A., and R. Mead. 1965. A simplex method for function minimization. Comput J **7**: 308–313.

Pinheiro, J. C., and D. Bates. 2002. Mixed-effect models in S and S-plus. Springer.

Pinheiro, J. C., D. Bates, S. DebRoy, D. Sarkar, and R. C. Team. 2020. nlme: Linear and nonlinear mixed effects models. R package version 3.1-144.

Potter, C., J. Melack, and D. Engle. 2014. Modeling methane emissions from Amazon floodplain ecosystems. Wetlands **34**: 501–511.

Praetzel, L. S. E., N. Plenter, S. Schilling, M. Schmiedeskamp, G. Broll, and K. H. Knorr. 2020. Organic matter and sediment properties determine in-lake variability of sediment CO2 and CH4 production and emissions of a small and shallow lake. Biogeosciences **17**: 5057–5078.

Ramirez, J. A., A. J. Baird, T. J. Coulthard, and J. M. Waddington. 2015. Testing a simple model of gas bubble dynamics in porous media. Water Resour. Res. **51**: 1036–1049.

Rodriguez, M., T. Gonsiorczyk, and P. Casper. 2018. Methane production increases with warming and carbon additions to incubated sediments from a semiarid reservoir. Inland Waters **8**(1): 109–121.

Scandella, B. P., C. Varadharajan, H. F. Hemond, C. Ruppel, and R. Juanes. 2011. A conduit dilation model of methane venting from lake sediments. Geophys. Res. Lett. **38**(6): https://agupubs.onlinelibrary.wiley.com/doi/full/10.1029/2011GL046768

Schmid, M., I. Ostrovsky, and D. F. McGinnis. 2017. Role of gas ebullition in the methane budget of a deep subtropical lake: What can we learn from process-based modeling? Limnol. Oceanogr. **62**: 2674–2698.

Segers, R. 1998. Methane production and methane consumption: A review of processes underlying wetland methane fluxes. Biogeochemistry **41**: 23–51.

Sieczko, A. K., and others. 2020. Diel variability of methane emissions from lakes. Proc Natl Acad Sci USA: 202006024. **117**(35): 21488–21494.

Smolders, A. J. P., L. H. T. Vergeer, G. van der Velde, and J. G. M. Roelofs. 2000. Phenolic contents of submerged, emergent and floating leaves of aquatic and semi-aquatic macrophyte species: Why do they differ? Oikos **91**: 307–310.

Sobek, S., and others. 2009. Organic carbon burial efficiency in lake sediments controlled by oxygen exposure time and sediment source. Limnol. Oceanogr. **54**: 2243–2254.

Stumm, W., and Morgan, J. 1996. Chemical equilibria and rates in natural waters. Aquatic chemistry, 3rd ed. Wiley.

Tranvik, L. J., and others. 2009. Lakes and reservoirs as regulators of carbon cycling and climate. Limnol. Oceanogr. **54**: 2298–2314.

Valentine, D. W., E. A. Holland, and D. S. Schimel. 1994. Ecosystem and physiological controls over methane production in northern wetlands. J. Geophys. Res. Atmos. **99**: 1563–1571.

van Hulzen, J. B., R. Segers, P. M. van Bodegom, and P. A. Leffelaar. 1999. Temperature effects on soil methane production: An explanation for observed variability. Soil Biol. Biochem. **31**: 1919–1929.

Vavilin, V. A., B. Fernandez, J. Palatsi, and X. Flotats. 2008. Hydrolysis kinetics in anaerobic degradation of particulate organic material: An overview. Waste Manag. **28**: 939–951.

West, W. E., J. J. Coloso, and S. E. Jones. 2012. Effects of algal and terrestrial carbon on methane production rates and methanogen community structure in a temperate lake sediment. Freshw Biol **57**: 949–955.

Yvon-Durocher, G., and others. 2014. Methane fluxes show consistent temperature dependence across microbial to ecosystem scales. Nature **507**: 488–491.

Acknowledgments

The research leading to these results has received funding from the European Research Council under the European Union's Seventh Framework Programme (FP7/2007-2013)/ERC grant agreement n° 336642. The authors thank Tadhg Moore for his help with the optimization process and Raquel Mendonça and Nathan Barros for commenting the manuscript. The authors have no conflicts of interest to declare.

Conflict of interest

None declared.

Submitted 20 January 2021
Revised 27 May 2021
Accepted 05 July 2021

Associate editor: Werner Eckert